STRUCTURAL DESIGN OF A GUIDING PLATE IN THE PLASTIC REGION

Author:

Fábio L. Amaral dos Anjos
Senior Engineer
phone: 55 11 886-2917
e-mail: f195.fe309@memo.daimler-benz.com

Co-authors:

Romulo R. Ripoli
CAE Supervisor
phone: 55 11 886-2767
e-mail: f195.fe303@memo.daimler-benz.com

Marcos Antonio Argentino
Engineering Manager
phone: 55 11 886-2778
e-mail: f195.fe300@memo.daimler-benz.com

Company:

debis humaitá IT Sevices Latin America
Alameda Campinas, 1070 - 10th fl. - Jd. Paulista
ZIP 01404-002 - São Paulo - SP - Brazil

ABSTRACT

In order to study the mounting stresses of a guiding plate which holds the leaf spring suspension of a bus, a structural finite element analysis, with MSC/NASTRAN v.70, was conducted. Plasticity and non-linear geometric effects was considered on the model.

The mounting load was evaluated and experimentaly measured. Results from the finite element model of the guiding plate were compared to experimental ones.

A new geometrical configuration for the part was suggested and analized. The aim was to minimize plastic deformation of the material and to reduce the mounting stresses.

1. Introduction

Plastic deformation is a time-independent permanent deformation. It is due to permanent changes in atomic positions of the material. It is not reversible and thus depends on the load history. Most metals exhibit this behavior at high stresses.

This paper shows a design study of a steel component that undergoes permanent deformation at mounting conditions. The component is a guiding plate which holds the leaf spring suspension of a bus. It is welded to the axle and conected to the leaf spring suspension by steel clamps (see figure 1).

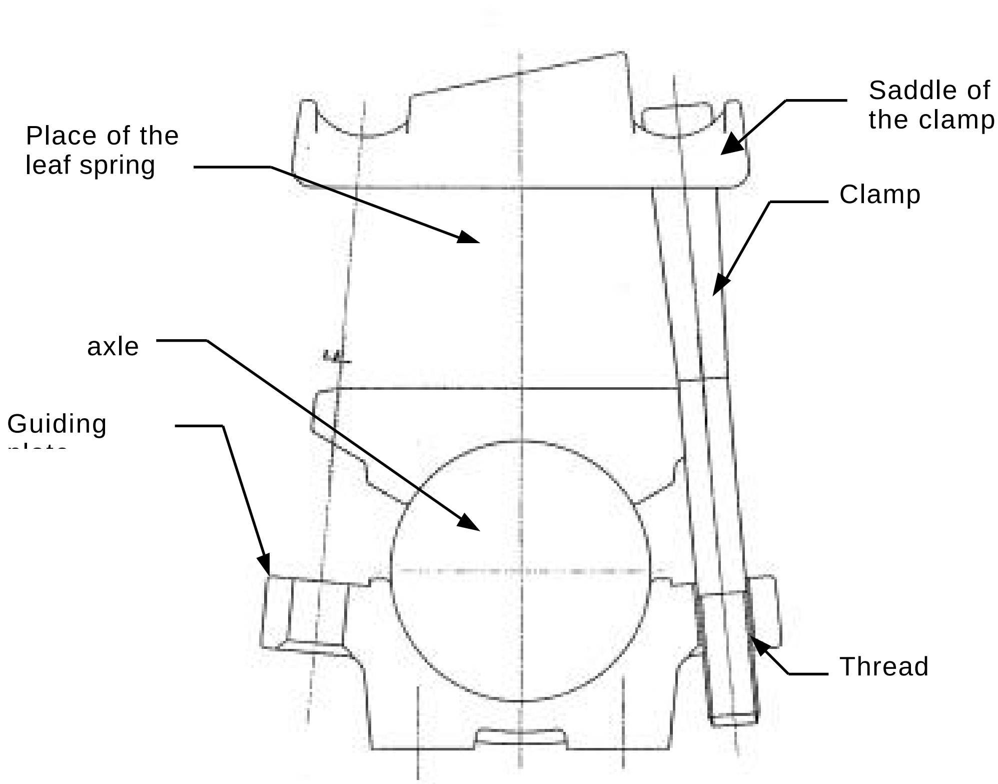

Fig. 1 - Layout of the leaf spring suspension.

2. Problem Definition

As known from the mounting process, the initial configuration of the guiding plate exhibits large deflection and permanent deformation. Large deflection is undesired since it may cause bending moment at the clamp. Permanent deformation means that the stress level is above the yield stress of the material, so it is important to know how far will be the maximum stress from the ultimate stress of the material. In this situation a tradicional linear structural finite element analysis will not be effectiv. Thus a non-linear structural analysis, considering plasticity and non-linear geometric, becomes necessary to investigate the stresses distribution in the guiding plate. This way we can follow the behavior of the part along the "stress ***x*** strain" curve of its material, even beyond yielding point, and then decide if this configuration is satisfactory or not.

Two diferent configurations were analised: the original one and a reinforced one that was modified taking into account the forging matrices used to create the first, i.e., the ideia was to reuse them to minimize costs.

2.1 Models

Figures 2 and 3 show the geometry of the original guiding plate. Due to symmetry only _ of the component (guiding plate) was analised. A tetrahedron mesh elements was automatic generated in the CATIA v4.1.8 package [1] (from Dassault Systèmes). The boundary conditions was applied in the MEDINA 6.1.5 software [2] (from Debis Systemhaus). The analysis were executed with MSC/NASTRAN v70 [3] (from The MacNeal-Schwendler Corporation) and the post-processing tasks were made in the MEDINA 6.1.5. In this case a 106 solution routine was used in MSC/NASTRAN.

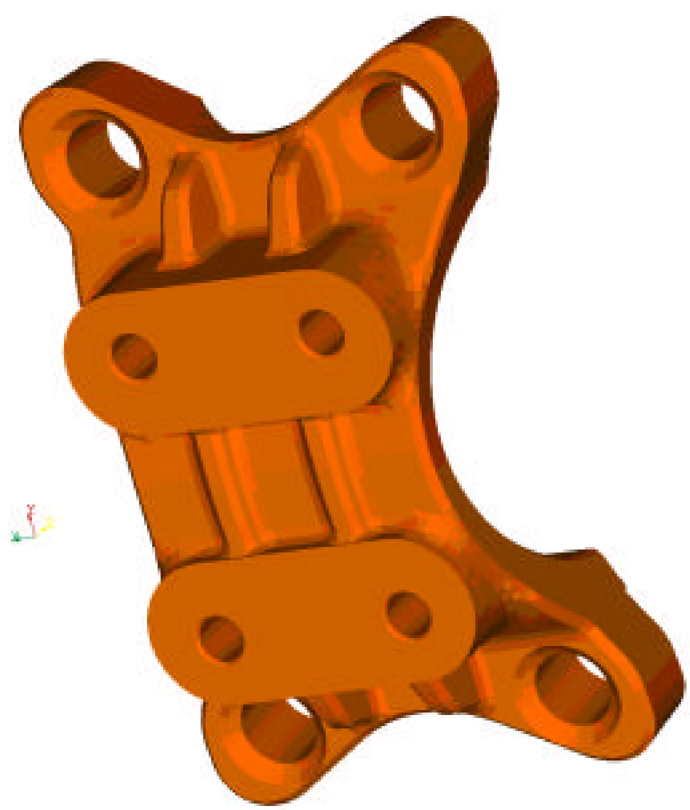

Fig. 2 - Geometry of the original guiding plate. View one (Bottom).

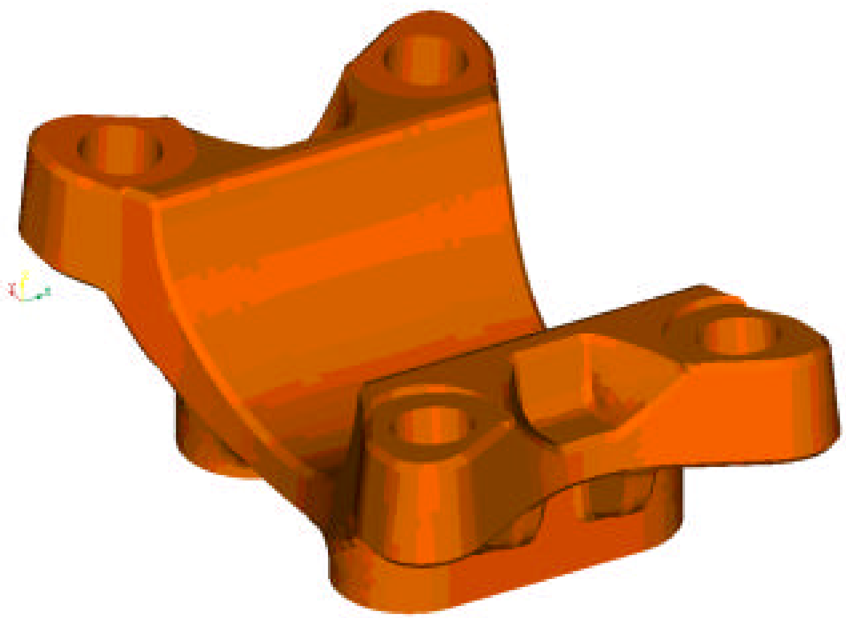

Fig. 3 - Geometry of the original guiding plate. View two (Top).

2.1.1 Original configuration

Figures 4 and 5 show the tetrahedron mesh generated for the original configuration.

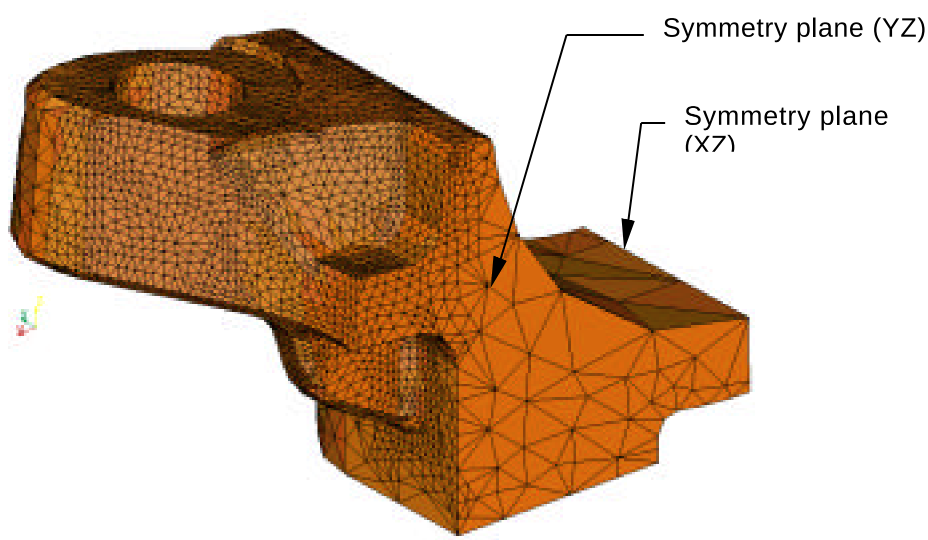

Fig. 4 - Finite element mesh of _ of the original guiding plate. Right view.

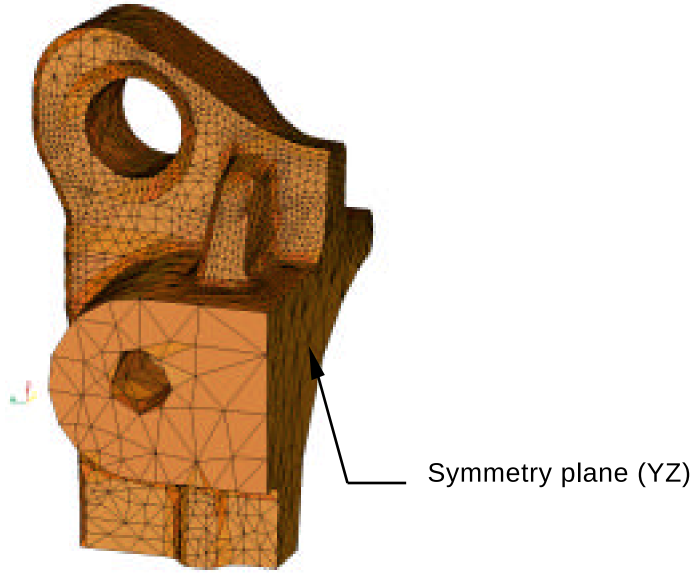

Fig. 5 - Finite element mesh of _ of the original guiding plate. Bottom view.

2.1.2 Reinforced configuration

Based on the original geometry some changes were made: increase the volume of the material at the hole contour; increase the length of the stiffener; removal of the milled seat; and filling of the cavity. This configuration is shown in figures 6 and 7.

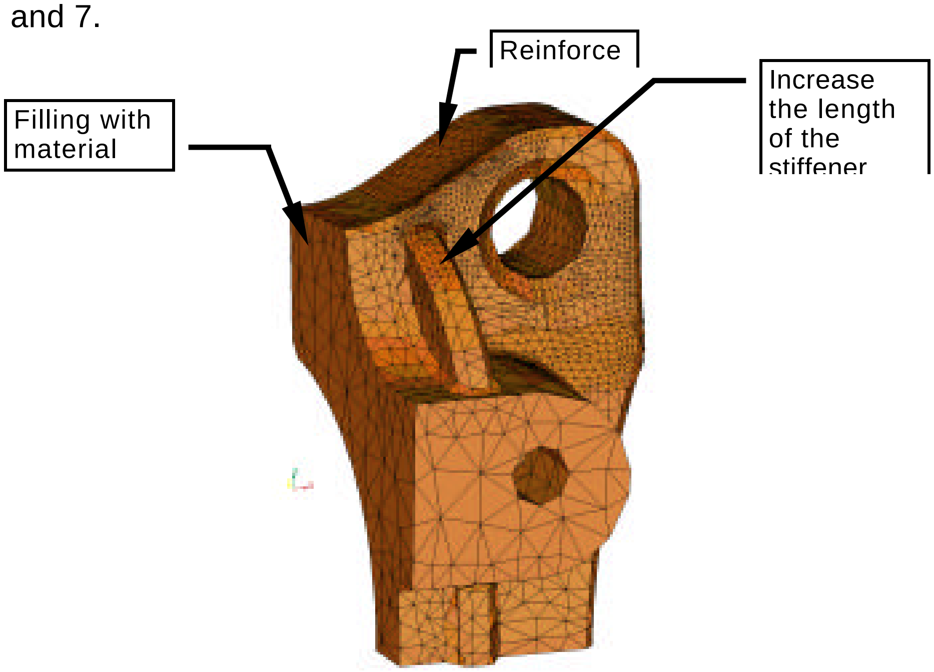

Fig. 6 - Finite element mesh of _ of the reinforced guiding plate. Bottom view.

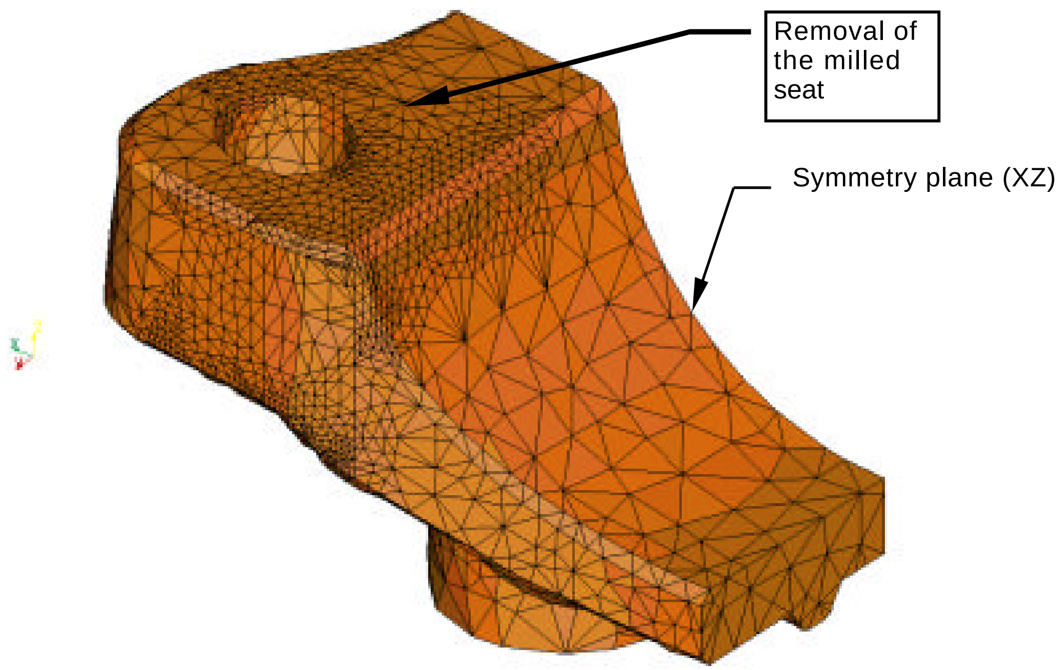

Fig. 7 - Finite element mesh of _ of the reinforced guiding plate. Isometric view.

2.2 LOADS

The first problem that rises is to obtain the actual force acting on the guiding plate. The mounting torque given at the nut, set at the clamp ends, has a predefined value of 750 Nm. Knowing the torque, the areas of contact between the nut and its seat on the guiding plate, the thread specifications, the materials, surface finishing and friction coeficients involved, the axial force on the clamp was evaluated using the methodology proposed by Niemann [4]. So the evaluated axial force is 25.8×10^3 kgf.

In order to get more reliable data about the axial force experimental tests were conducted. At these experiences the torque was slowly and manualy increazed with 50 Nm incremments at the same time the deformation of the clamp was measured by strain gauges. In fact the strain-gauges reading was calibrated to give the axial force on the clamp rod. The experimental results showed that the axial force vary between 21.75×10^3 kgf and 28.25×10^3 kgf. So we can see good agreement between experimental and analytical force values.

The dynamic axial force on the clamp was evaluated using a multi-body system software (ADAMS 8.2 [5] from Mechanical Dynamics Inc.). It was found a maximun dynamic axial force of 1.75×10^3 kgf, value much smaller than the mounting one.

In the FE model, the axial force from de clamp was distributed at nodes on the nut's seat surface on the guiding plate.

2.3 Boundary conditions

Symmetry conditions were applied at nodes on the two symmetry planes, and a fixed condition was applied at nodes at axle-welded region.

2.4 Material properties

The material used for the guiding plate is the St-52 3N. Some mechanical properties of this material are shown in table 1, and a "stress ***x*** strain" curve is shown in figure 8

Table - 1: Mechanical properties of the St-52 3N.

Material	**Yield stress (N/mm^2)**	**Ultimate stress (N/mm^2)**	**Poisson's ratio**	**Young's modulus (N/mm^2)**
St-52 3N	355	530	0.3	210000

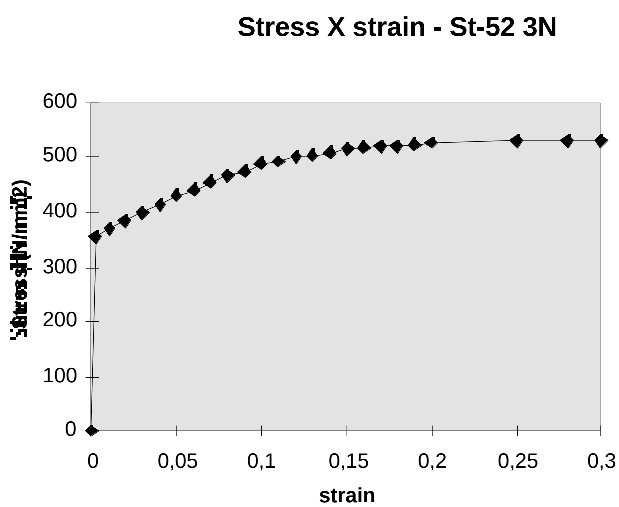

Fig. 8 - Stress ***x*** strain curve for St-52 3N.

3. Analysis

The results from the MSC/NASTRAN's 106 solution routine are shown in figure 9 to figure 14. The post-processing tasks were made in the MEDINA 6.1.5.

3.1 Original configuration

Figures 9 and 10 show the von Mises stress distribution for this case. The applied force is 25.8×10^3 kgf. The maximum displacement resulted was 6.11 mm at the fixing tip.

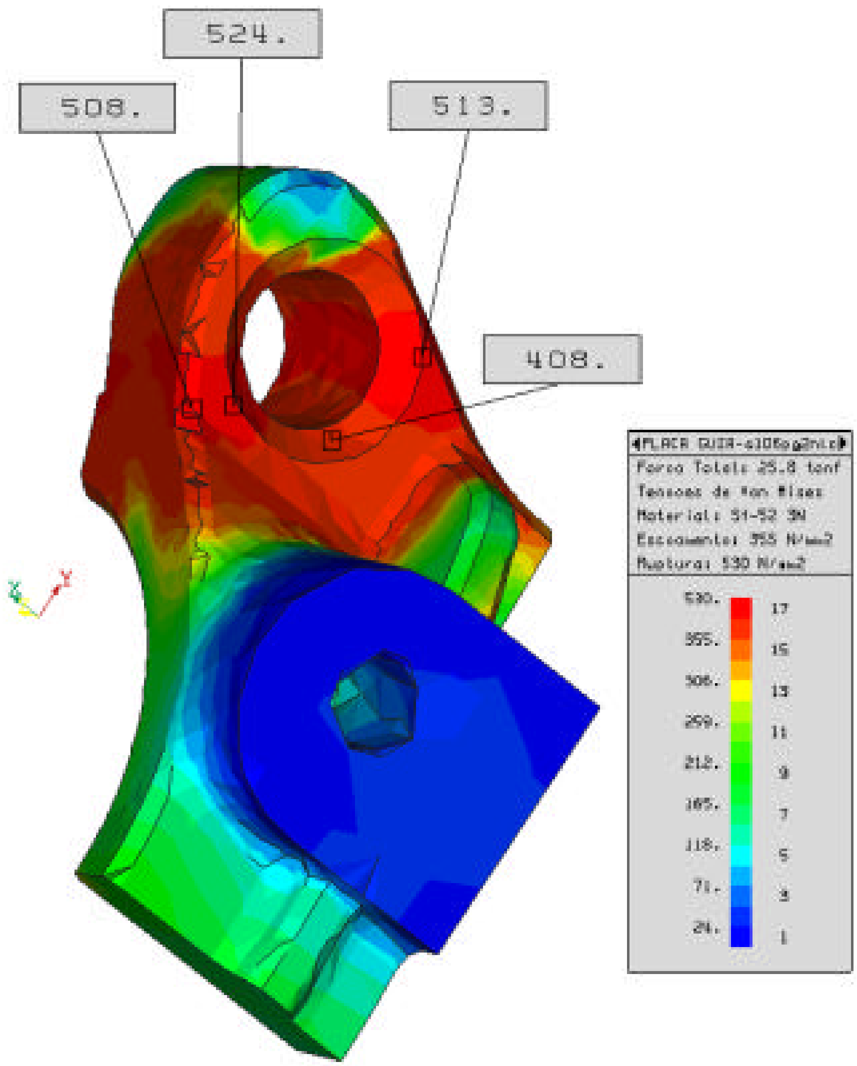

Fig. 9 - Von Mises stress distribution in the original configuration. Force= 25.8×10^3 kgf. Bottom view. Stresses in red are above yield stress.

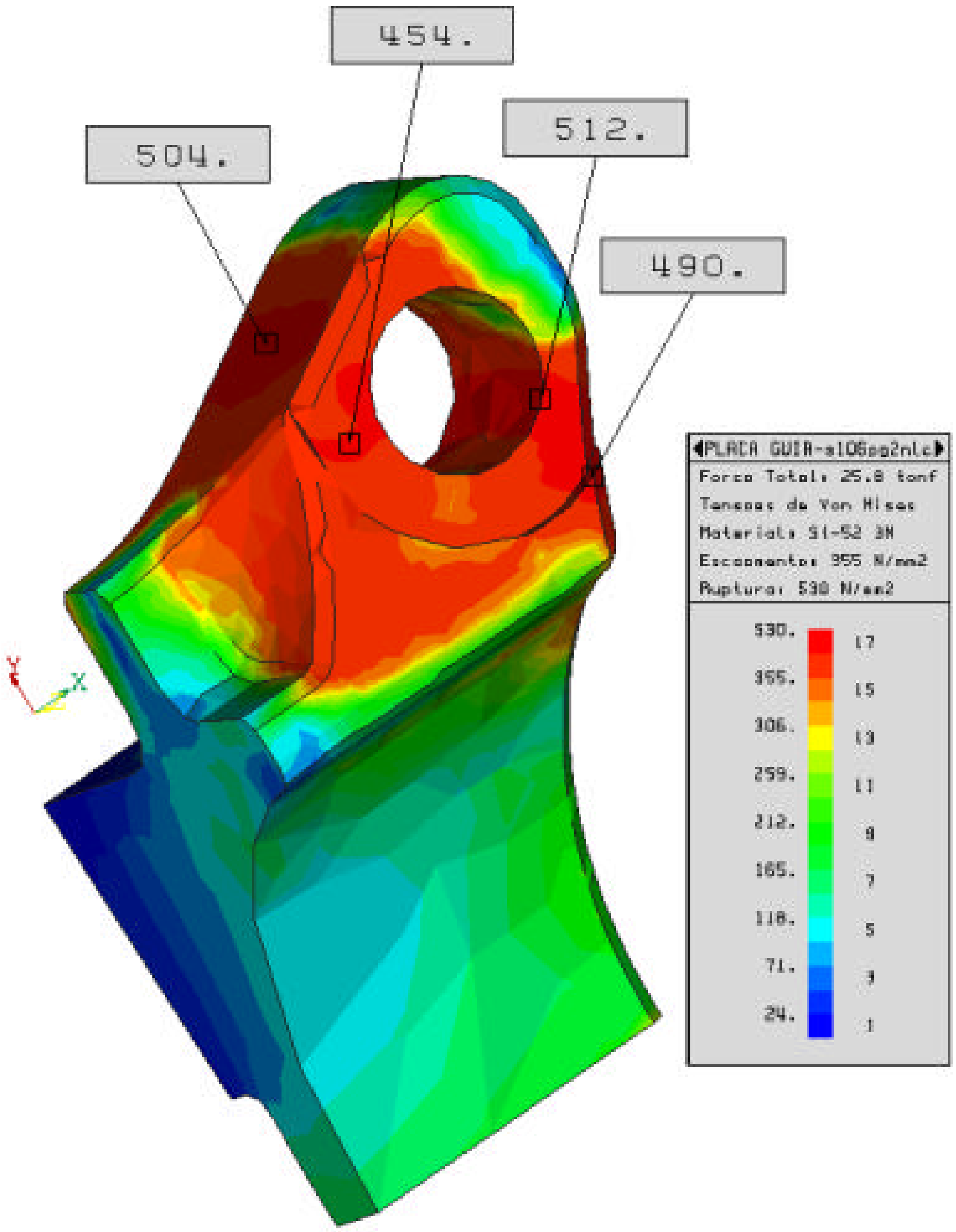

Fig. 10 - Von Mises stress distribution in the original configuration. Force= 25.8x10^3 kgf. Top view. Stresses in red are above yield stress.

3.2 Reinforced configuration

Figures 11 and 12 show the von Mises stress distribution for the reinforced configuration with an applied force of 25.8×10^3 kgf, while figures 13 and 14 show the same configuration under a force of 30.0×10^3 kgf. For the first load case the maximum displacement at the fixing tip was 0.204 mm and for the second, it was 0.232 mm.

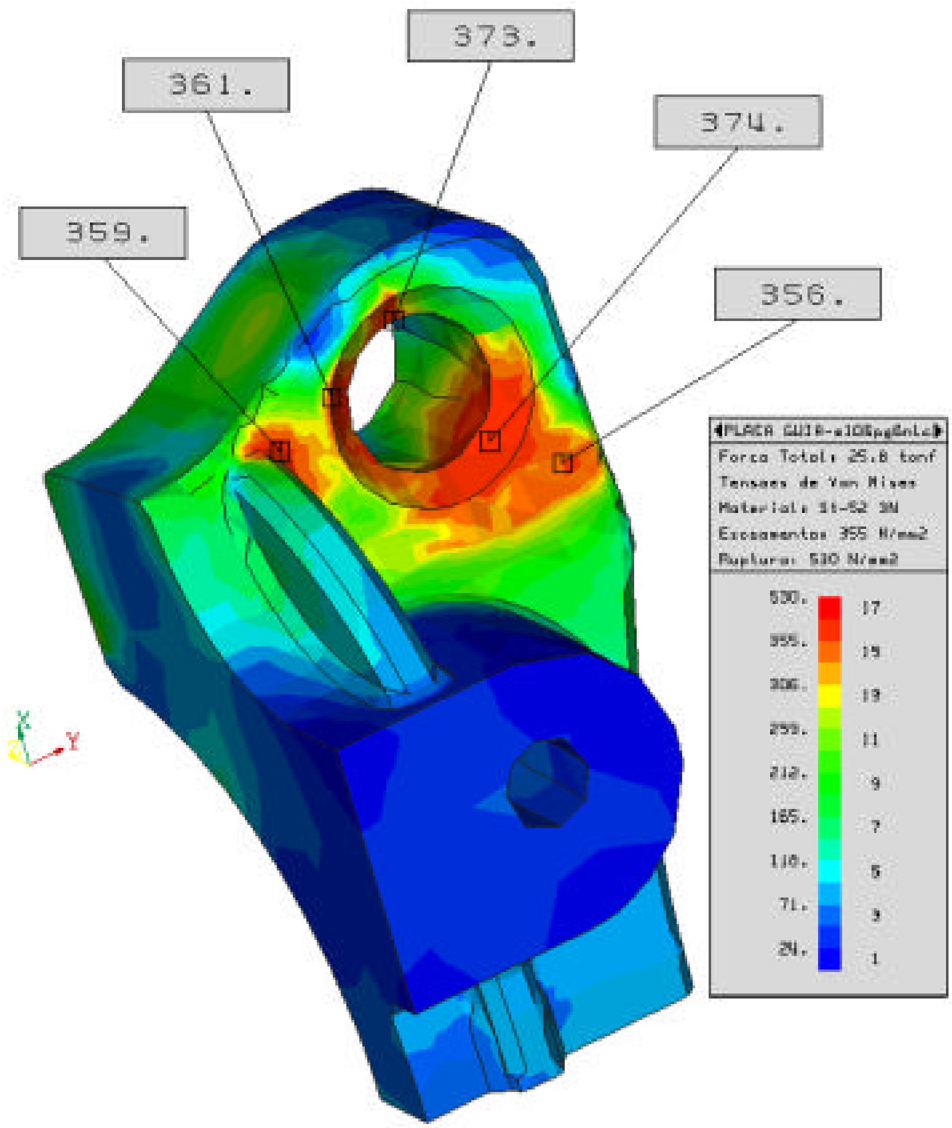

Fig. 11 - Von Mises stress distribution in the reinforced configuration. Force= 25.8×10^3 kgf. Bottom view. Stresses in red are above yield stress.

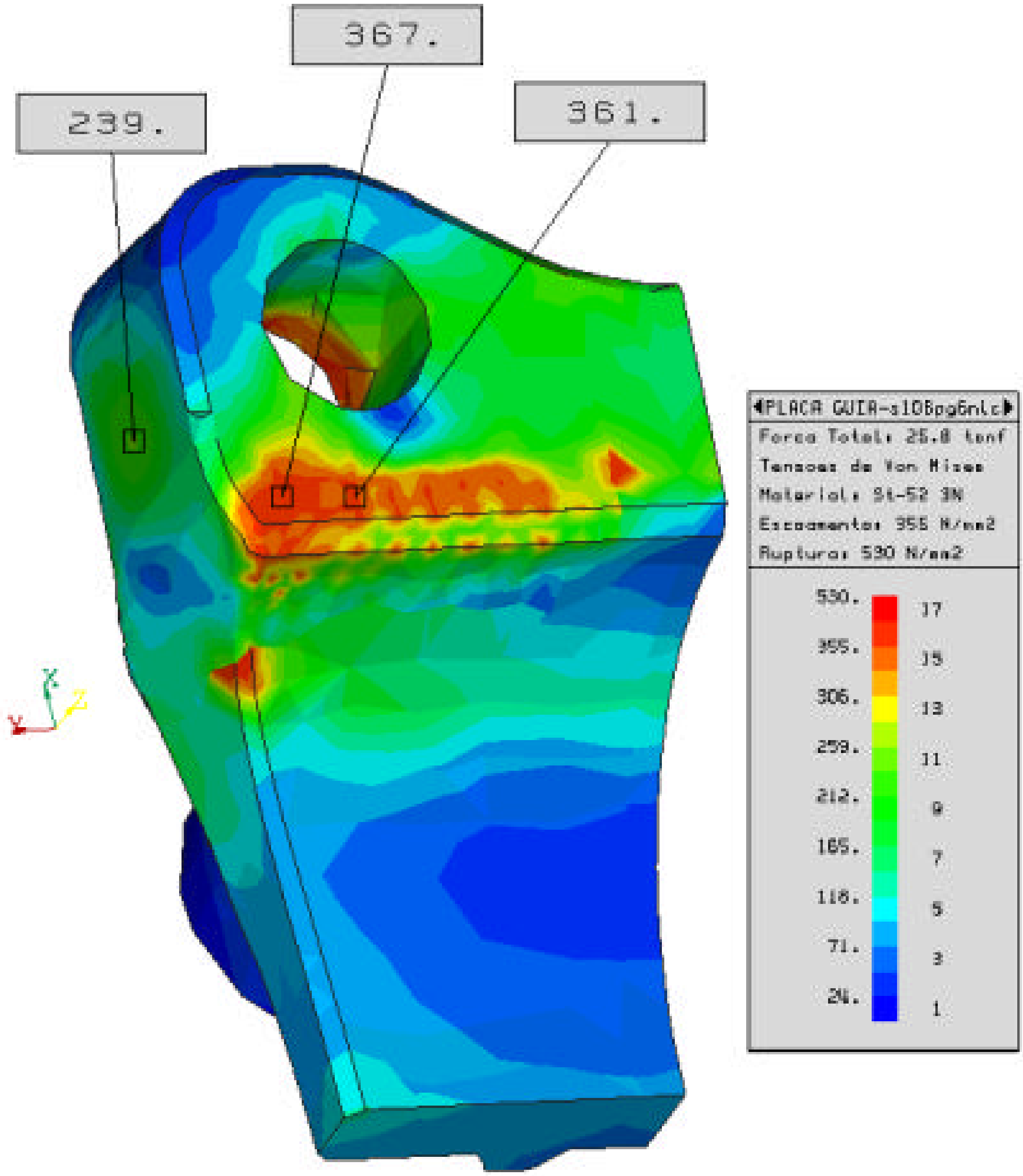

Fig. 12 - Von Mises stress distribution in the reinforced configuration. Force= 25.8×10^3 kgf. Top view. Stresses in red are above yield stress.

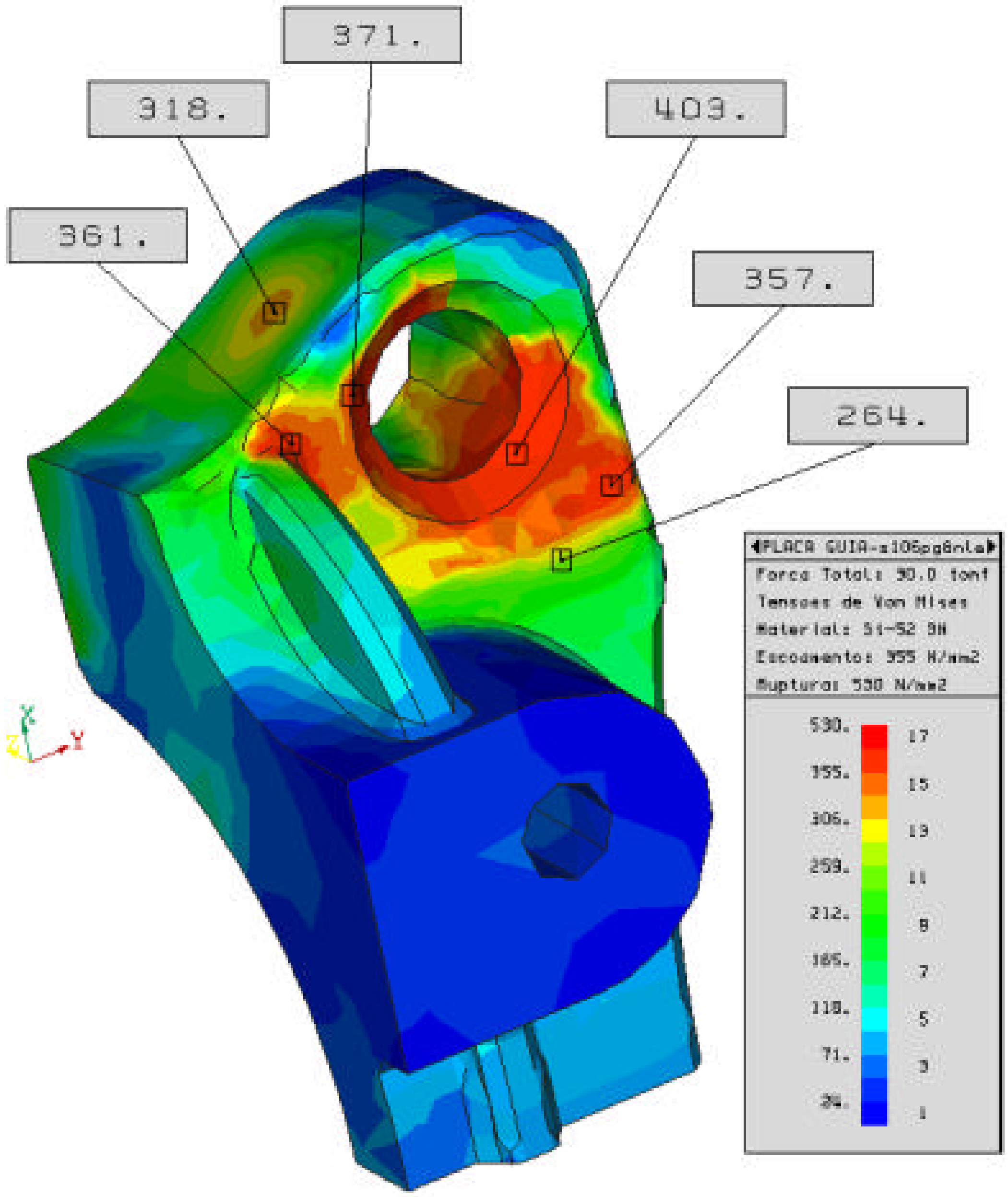

Fig. 13 - Von Mises stress distribution in the reinforced configuration. Force= 30.0×10^3 kgf. Bottom view. Stresses in red are above yield stress.

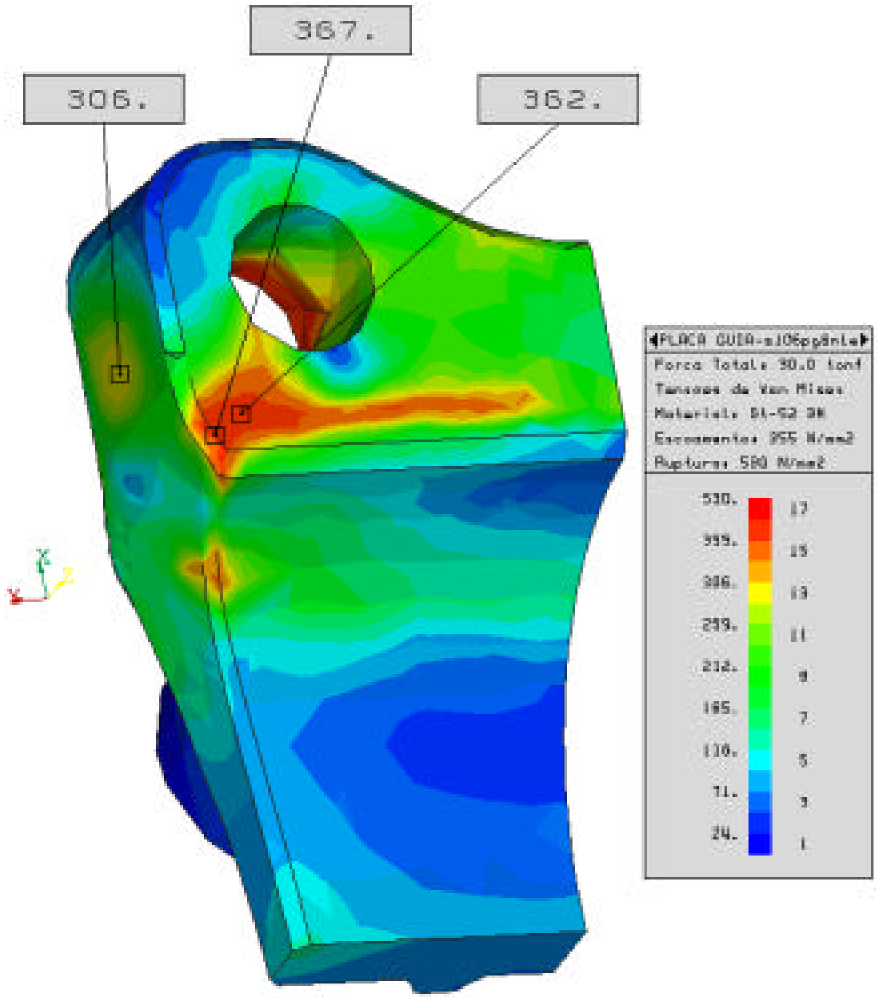

Fig. 14 - Von Mises stress distribution in the reinforced configuration. Force= $30.0\text{x}10^3$ kgf. Top view. Stresses in red are above yield stress.

4. Discussions

The calculated axial force on the clamp rod shows good agreement with the experimental ones.

We can see in figures 9 and 10 that the original configuration have a big area under plastic behavior, so the large deflection at the fixing tips (6.11 mm). In this case one experimental measurement showed a 4.0 mm residual deformation for this point. As the axial force may vary from $21.75\text{x}10^3$ kgf to $28.25\text{x}10^3$ kgf, the calculated deflection agree very well with reality. The difference may be due to the actual presence of the clamp, that is not considered in the finite element models.

Figures 11, 12, 13 and 14 show a small area under plastic deformation for the reinforced case. The deflection at fixing tip is small too, only 0.232 mm for a 30.0×10^3 kgf.

Both configurations have plastified regions when a 25.8×10^3 kgf force is applied, but the original one has a maximum stress of 524 N/mm^2, value that is too close from the ultimate stress of the material (530 N/mm^2). So the risk of break during the mounting process is iminent. The deflection of the fixing tip was so large too (6.11 mm), inducing bending moment at the clamp.

Though the reinforced configuration exhibits plastic deformations, the maximum stress of 374 N/mm^2, when the applied force is 25.8×10^3 kgf, is suficiently far from the ultimate stress of the material.

Even considering a critical situation, where the applied force reaches 30.0×10^3 kgf (adding the dynamics effects), the maximum stress (403 N/mm^2) is suficiently bellow from the ultimate stress, providing that this configuration will not break statically.

More detailed analysis could be done considering contact elements between the guiding plate and the clamp rod. This way we can get even more precise results.

5. Conclusions

The original configuration exhibits large deflection and high stress, close to the ultimate stress of the material. So it is not recomended for this application.

The reinforced configuration exhibits small deflection and, though there are plastic deformations, the maximum stress for a critical situation is suficiently bellow from the ultimate stress of the material. So this new configuration could be used for this application.

With this work it was possible to find a new guiding plate configuration that fulfil some predefined constraints, like available space, reuse the forging matrices and keep the same material of the original part. All without constructing any prototype.

6. Acknowlegements

The authors wish to thank Mercedez-Benz do Brasil for authorization for publishing this paper and for the experimental tests done.

7. References

[1] CATIA Finite Element Modeler Interactive Functions User´s Reference Manual v.4.1.9, Dassault Systèmes, 1997.

[2] debis-MEDINA Postprocessing, version 6.0 Reference Manual, debis Systemhaus Engineering Gmbh, 1996.

[3] MSC/NASTRAN User's Manual, Version 70, The MacNeal-Schwendler Corporation, Los Angeles, CA., 1997.

[4] Niemann, G., Elementos de Máquinas, Vol. I, Translated by Langendonck, C. and Rehder, O. A., Ed. Edgard Blücher Ltda., São Paulo, 1971.

[5] ADAMS/VIEW User´s Reference Manual, version 8.0, Mechanical Dynamics, Ann Arbor, MI, 1994.